Variable Termination Unit for Noise-Parameter Measurement

Dazhen Gu, *Member, IEEE*, David K. Walker, *Senior Member, IEEE*, and James Randa, *Senior Member, IEEE*

***Abstract*—The National Institute of Standards and Technology (NIST) has upgraded its capability to measure noise parameters on low-noise amplifiers with a variable termination unit (VTU) in the frequency range of 1–12.4 GHz. Such a unit allows improved time efficiency and accuracy in the noise-temperature measurements used to de-embed the noise parameters of amplifiers. We present the design and characterization of the VTU. The measured results of one particular amplifier at integer frequencies ranging from 8 to 12 GHz show satisfactory accuracy. The VTU method is also validated by comparison with the results from the manual method.**

***Index Terms*—Amplifier noise parameters, noise measurement, source pull technique, uncertainty analysis.**

I. Introduction

RAPID developments on low-noise amplifiers (LNAs) have generated interest and the need for accurate measurements of noise properties [1]–[3]. In general, amplifier noise is measured using the Y-factor method under the condition of 50-Ω termination. However, the determination of IEEE noise parameters (minimum noise temperature $T_{\min}$, noise resistance R_n, and optimal complex reflection coefficient of the source Γ_{opt}) reveals intrinsic noise properties and is of more practical importance, particularly for bare transistors [4].

The National Institute of Standards and Technology (NIST) has established the capability to measure noise parameters for both packaged LNAs [5] and on-wafer LNAs and transistors [4]. We adopted a source-pull approach that varies the impedance seen at the input of the amplifier. Previous measurements of noise parameters at NIST were very time consuming, owing mainly to the manual connection and disconnection of different terminations. To expedite the measurement, we have recently designed and built a variable termination unit (VTU), allowing automated switching to multiple input impedance states and both ambient and nonambient temperature terminations for the amplifier under test.

In addition to the manual and VTU methods, there are other alternatives for producing multiple impedance states. Automated tuner systems have widely been used in load- or source-pull measurements in the microwave design and manufacturing industry. A tuner system can provide excellent coverage on the entire Smith chart at its operating frequencies. However, tuners often exhibit poor repeatability and require real-time measurement of the impedance [2]. This leads to sophisticated metrology architecture, including extra components, such as low-loss couplers and highly repeatable switches, and a vector network analyzer (VNA). Electronic calibration modules are another possible option. They were originally designed for single-connection VNA calibration to reduce errors arising from mechanical connections. The electronic calibration module can be programmed to output a limited number of impedance states, which are predefined by the manufacturer. Although the electronic calibration module can potentially be used as a compact and programmable multiple impedance provider, its repeatability, in terms of the reflection coefficient and output noise, is presently unknown. In addition, highly reflective impedance states are difficult to achieve from the electronic calibration module, particularly at higher frequencies.

In this paper, we present the newly designed VTU as an extended work to our previous short report [6]. The new version of the VTU inherits the basic design concept of the old version and bears a few improvements that we intended to make in [6]. A detailed design consideration of the VTU, including termination choices, thermal stability, and vibration control, is described in Section II. Section III shows the characterization of the VTU, in terms of its impedance mapping and repeatability check. A packaged amplifier operating in the frequency range of 8–12 GHz was measured with the VTU, and the results are presented in Section IV. Some discussions and conclusions are given in Section V.

II. Design of VTU

The VTU consists of three switches, i.e., one two-way switch (first stage, SW1) in connection with two identical six-way in-line switches (second stage, SW2A and SW2B), as shown in Fig. 1. All the switches are electromechanical for low loss and highly repeatable performance. In addition, unlike their solid-state counterpart, electromechanical switches are passive components; therefore, the added noise contributed by them to the system is well known.

The common port of the two-way switch is connected to a PC-3.5-to-PC-7 adapter, which serves as the output of the VTU. Port 1 of SW1 is connected to the common port of SW2A through an SMA adapter, which consists of two L-shaped connectors. Port 2 of SW1 is connected to the common port of SW2B in the same manner. The SMA adapter is used to release

Manuscript received June 6, 2008; revised September 9, 2008. First published November 18, 2008; current version published March 10, 2009. The Associate Editor coordinating the review process for this paper was Dr. Tae-Weon Kang.

D. Gu and D. K. Walker are with the Electromagnetics Division, National Institute of Standards and Technology, Boulder, CO 80305 USA (e-mail: dazhen.gu@boulder.nist.gov).

J. Randa is with the Electromagnetics Division, National Institute of Standards and Technology, Boulder, CO 80305 USA, and also with the Department of Physics, University of Colorado at Boulder, Boulder, CO 80309 USA.

Digital Object Identifier 10.1109/TIM.2008.2007055

0018-9456/$25.00 © 2008 IEEE

Authorized licensed use limited to: NIST Researchers. Downloaded on May 11, 2009 at 18:27 from IEEE Xplore. Restrictions apply.

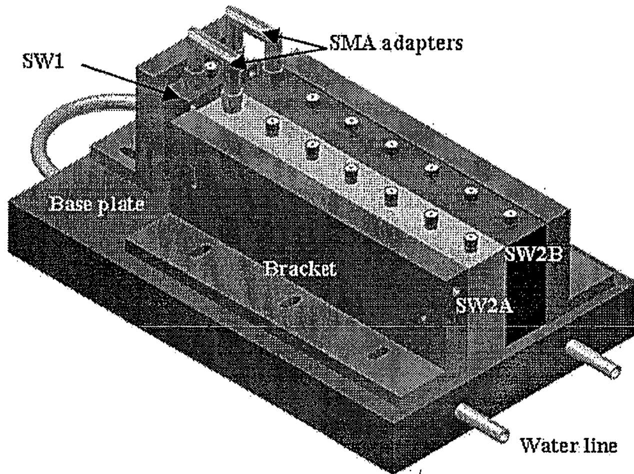

Fig. 1. VTU architecture. The 12 ports are available for device terminations to provide multiple impedance states and different input noise powers. The entire unit is housed in an aluminum enclosure.

any mechanical stress due to the connection since the closest distance between the common ports of SW2A and SW2B is slightly larger than the separation between ports 1 and 2 of SW1. A total of 12 ports of SW2A and SW2B are available for device terminations.

A. *Choice of Terminations*

The choice of terminations is somewhat arbitrary. As long as the VTU provides no fewer than four different impedance states, the four noise parameters can numerically be solved by fitting. However, keeping some criteria in mind, we can minimize the propagation of measurement errors and ensure sufficient data redundancy.

The effective noise temperature as a function of the source reflection coefficient can be represented as

$$T_e = T_{\min} + \frac{4R_nT_0}{Z_0}\frac{|\Gamma_{\text{opt}} - \Gamma_S|^2}{|1+\Gamma_{\text{opt}}|^2(1-|\Gamma_S|^2)} \quad (1)$$

where Γ_S is the reflection coefficient of the source; Z_0 is the reference impedance, which is nominally 50 Ω; and $T_0 =$ 290 K. To simplify the discussion, we express (1) in terms of the source admittance $Y_S = G_S + jB_S$, i.e.,

$$T_e = T_{\min} + \frac{R_nT_0}{G_S}|Y_{\text{opt}} - Y_S|^2. \quad (2)$$

By taking the first-order derivative of (2) and assuming a first-order approximation that the errors between the four noise parameters are uncorrelated, we obtain the following expression:

$$\begin{aligned}\Delta T_e = {} & \Delta T_{\min} + \frac{T_0}{G_S}|Y_{\text{opt}} - Y_S|^2 \times \Delta R_n \\ & + \frac{2R_nT_0}{G_S}(G_{\text{opt}} - G_S) \times \Delta G_{\text{opt}} \\ & + \frac{2R_nT_0}{G_S}(B_{\text{opt}} - B_S) \times \Delta B_{\text{opt}}. \end{aligned} \quad (3)$$

Equation (3) offers useful information on the selection of appropriate input sources. Regardless of any input source impedances, the measurement error has the same impact as the error for $T_{\min}$. However, the use of admittance states closer to the optimal value Y_{opt} results in augmented errors of R_n, G_{opt}, and B_{opt}. To keep the uncertainty in noise parameters small, we prefer to use mostly the admittance states that are not close to Y_{opt}.

The impedance is usually well matched for a packaged amplifier. Therefore, highly reflective devices would be good candidates for the input termination of packaged amplifiers in noise-parameter measurements. On the other hand, bare transistors lack input-matching networks and may therefore require different types of terminations to minimize the uncertainty of all noise parameters. As the main focus of this paper, the VTU design for the noise-parameter measurement of packaged amplifiers will be discussed.

In addition to the individual impedance values, the overall impedance coverage of the VTU on the Smith chart is also essential. Because the paired ports on the two six-way switches (for example, the first port of SW2A and the first port of SW2B) have approximately the same physical length from the reference plane, they should be closely phase matched. To obtain wide coverage, we use open and short pairwise configurations on the first four ports of SW2A and SW2B, resulting in impedances of nearly 180° apart for paired ports. In other words, the first four ports of SW2A are occupied by opens, whereas the first four ports of SW2B are occupied by shorts. The rest of the ports are organized as follows: The fifth port of SW2A is terminated by an SMA short in connection with a 3-dB attenuator, the fifth port of SW2B is terminated by a matched load, and the sixth ports of SW2A and SW2B are left for external device connections, such as noise diodes and cold sources (normally a reverse-configured LNA).

B. *Temperature Stabilization and Vibration Control*

The output noise power of passive components is proportional to their physical temperature. The old VTU was found to be unstable temperaturewise [6]. The newly designed VTU incorporates a temperature-regulation feature. All the components are mounted on a water-cooled fixture, and the entire unit is housed in an enclosure with electronic interfaces and water line hookups. In addition, the switches are unbiased most of the time to prevent heat dissipation, except for a short time period during port switching. A calibrated thermistor is integrated inside the VTU to provide real-time temperature monitoring.

We also experienced mechanical vibration problems on the old VTU when the contact was toggled from one port to another. The vibration translated the movement to the external connector, resulting in reduced repeatability and measurement inaccuracy. This problem is particularly crucial in the on-wafer environment since the probe contact on the substrate can easily break due to mechanical vibration. All the switches in the new VTU are securely clamped to solid brass brackets that are all mounted on a massive water-cooled base plate. Clamp stiffness produces a mechanical restraint that diminishes the vibration.

Authorized licensed use limited to: NIST Researchers. Downloaded on May 11, 2009 at 18:27 from IEEE Xplore. Restrictions apply.

During the measurements, we also set a dwell time after each toggling before the data are measured.

The vibration is greatly reduced for the newly designed VTU, and the temperature fluctuation of the components is within the range of ± 0.05 K at the regulated temperature ($\sim$296 K).

III. Characterization of VTU

The VTU was characterized on a VNA in the frequency range of 1–12.4 GHz. The VNA was calibrated using the two-port thru–reflect–line (TRL) method [7] in the frequency range of 2–12 GHz and the one-port short–open–load method in the frequency range of 1–2 GHz. Appropriate power levels must be taken into account when probing the reflection coefficient of the VTU terminations. In particular, a low power level ($-35 \sim -40$ dBm) must be used for the cold source in order not to distort the low-level linear response of the LNA.

A. Phase Match

The VTU is constructed using identical paired parts, such as adapters and six-way switches. We expected a good phase match along the paired ports. However, the characterization of the VTU showed a clear phase difference over the entire frequency range for all paired ports. The phase difference of the first four pairs was less than 20° below 8 GHz and became as large as 40° at about 11 GHz.

The total phase difference can be broken down to the contributions from the SMA adapters, ports 1 and 2 of SW1, and two SW2s. We checked each part by individually measuring them. We found that most of the phase difference came from the two SMA adapters that linked SW1 to SW2s. For example, SMA adapters counted for 74% of the total phase difference at 8 GHz. They appeared even more poorly phase matched at higher frequencies. In principle, PC-3.5 adapters will provide a better phase match than SMA adapters. However, L-shaped adapters are not practically available in the PC-3.5 format.

B. Impedance Constellation

Although the phase match of paired ports was below our expectation, the impedance mapping of the VTU on the Smith chart is of more practical interest. The reflection coefficients of all terminations were measured at the reference plane (the output PC-7 connector) using the TRL-calibrated VNA.

We made various arrangements by using paired PC-3.5 adapters of different lengths connecting short and open terminations to the ports to adjust the phase delay between paired ports. We were able to acquire impedance coverage of four quadrants on the Smith chart at all the integer frequencies in the frequency range of 1–12 GHz, which will provide sufficient redundancy for noise-parameter simulation. A constellation of reflection coefficients at 9 GHz is shown in Fig. 2.

The impedance coverage could be improved at any specific frequency by inserting an adjustable airline between the switch port and the termination for phase delay fine tuning. However, we have not done so, because we are more interested in the broadband performance: Better coverage at one frequency may cause poor coverage at others.

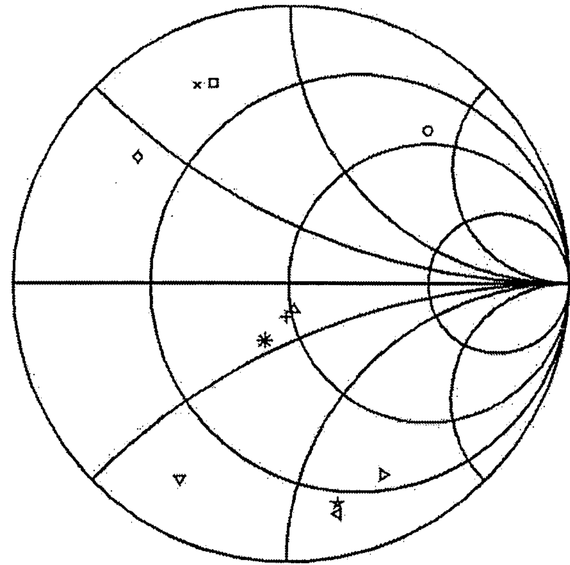

Fig. 2. VTU impedance constellation at 9 GHz. The impedance states of 12 terminations show good coverage on four quadrants of the Smith chart. Most of the impedances are far from the match point, which meets the design criteria for packaged amplifier characterization.

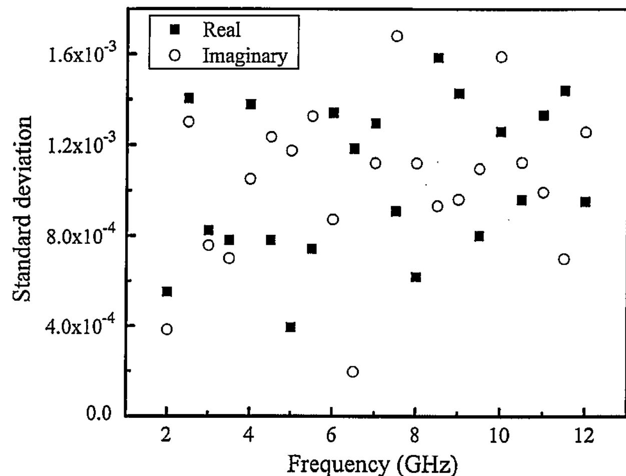

Fig. 3. Standard deviation of the complex reflection coefficients of termination 3 of the VTU for a total of 25 measurements in five different days. The standard deviations of all the VTU terminations are below 0.003, which is an indication of good repeatability.

C. Repeatability

The VNA was offline during the noise-parameter measurements in our VTU setup, unlike a tuner system. The data files of the reflection coefficients previously taken on the VNA were used for noise-temperature measurement. Therefore, the measurement accuracy heavily relies on the repeatability of the VTU. We performed a thorough repeatability check to gain knowledge and assurance of the VTU performance.

The VTU was toggled to each port five times, and the complex reflection coefficients were measured for each port.

Authorized licensed use limited to: NIST Researchers. Downloaded on May 11, 2009 at 18:27 from IEEE Xplore. Restrictions apply.

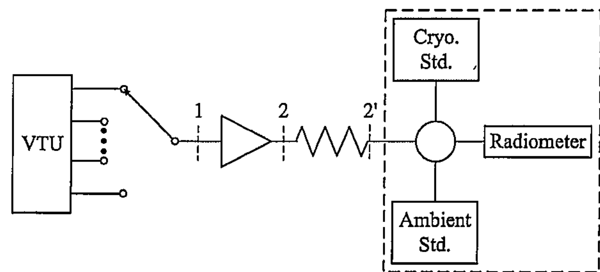

Fig. 4. Noise-temperature measurement setup. The components in the dashed box represent part of the NIST NFRad system.

Temperature regulation was enforced the entire time during the measurements. The standard deviation was below 0.001 for both the real and imaginary parts of the reflection coefficients for all terminations, except the cold source. As mentioned earlier, we were forced to apply much less incident power while measuring the cold source. The reflected power would even be lower due to the good port match of the cold source. This led to power sensing close to the bottom of the dynamic range of the VNA samplers, resulting in more random noise.

The same procedure was repeated for five days, and all data sets were analyzed, showing a standard deviation of below 0.003 (1σ) for all terminations, including the cold source. The standard deviation as a function of frequency for one particular termination (termination 3) is shown in Fig. 3. The positive result of this repeatability check lends confidence in the implementation of the VTU in noise-parameter measurements.

IV. Noise-Parameter Measurement and Fit

A. Measurement Setup

The setup of noise-parameter measurements on a packaged LNA operating in the frequency range of 8–12 GHz is shown in Fig. 4. The NIST NFRad system was used as the noise power measurement instrument [8]. The known noise temperature of the ambient and cryogenic standards defines the reference for the noise temperature of the LNA under test.

A 26-dB attenuator was inserted between the LNA and the radiometer to ensure that the NFRad system operated in its linear region. Prior to the noise-parameter measurement, the reflection coefficients at planes 1, 2, and $2'$ for each termination of the VTU were measured on the VNA, and all the data were transferred to the personal computer that controls the NFRad. The input noise temperatures at plane 1 for all nonambient terminations, such as the noise diode and the cold source, were measured first. Next, the output noise temperature at plane $2'$ was consecutively read 40 times for all 12 VTU terminations connected to plane 1. The noise temperature at plane 2 can be inferred from the output noise available at plane $2'$ by the knowledge of the available gain of the attenuator. In addition to the forward configuration, the LNA input was connected to the NFRad system, with its output terminated with an ambient matched load, to measure the reverse radiation from the LNA input.

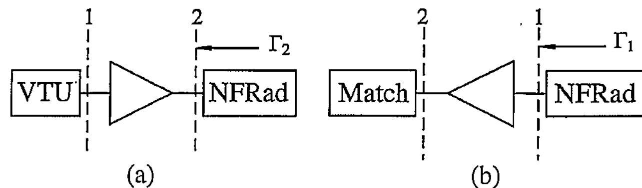

Fig. 5. LNA noise-parameter measurement arrangements. (a) Forward and (b) reverse configurations.

B. Noise-Parameter Fit

The general theoretical framework of the noise-parameter fit is outlined in [4]. We use the wave representation [9] to model the noise parameters of a linear two-port device, such as an amplifier. For convenience, we express the output noise temperature in terms of X parameters, which are directly associated with the intrinsic noise wave of the amplifier. The noise temperature for the forward and reverse configurations is given by

$$T_2 = \frac{|S_{21}|^2}{(1-|\Gamma_2|^2)} \left\{ \frac{(1-|\Gamma_S|^2)}{|1-\Gamma_S S_{11}|^2} T_S + \left| \frac{\Gamma_S}{1-\Gamma_S S_{11}} \right|^2 X_1 + X_2 + 2\mathrm{Re}\left[\frac{\Gamma_S X_{12}}{1-\Gamma_S S_{11}} \right] \right\} \quad (4)$$

$$T_1 = \frac{1}{(1-|\Gamma_1|^2)} \left\{ \frac{|S_{12}|^2 (1-|\Gamma_S|^2)}{|1-\Gamma_S S_{22}|^2} T_S + X_1 + \left| \frac{S_{12} S_{21} \Gamma_S}{1-\Gamma_S S_{22}} \right| X_2 + 2\mathrm{Re}\left[\frac{S_{12} S_{21} \Gamma_S X_{12}^*}{1-\Gamma_S S_{22}} \right] \right\} \quad (5)$$

respectively, where the S_{ij}'s are the S-parameters of the LNA, and Γ_S and T_S are the source reflection coefficient and source noise temperature, respectively. Γ_2 represents the reflection coefficient at plane 2 for the forward configuration, as shown in Fig. 5(a), and Γ_1 represents the reflection coefficient at plane 1 for the reverse configuration, as shown in Fig. 5(b).

Equations (4) and (5) are basic formulas used in the fitting program. In addition to four noise parameters [X_1, X_2, $\mathrm{Re}(X_{12})$, and $\mathrm{Im}(X_{12})$], the reduced gain, which is defined by $G_0 \equiv |S_{21}|^2$, can be computed as an unknown variable. The fit is insensitive to the phase of S_{21}, as an immediate result of (4) and (5), where the considerably small value of S_{12} keeps the terms consisting of S_{21} negligible. First, we perform a fit on the data from the measurements of the forward configuration. The unknown variables can be redefined, and the problem can be solved in a manner of linear least-square fitting. Next, the acquired values are considered as a set of starting seeds of nonlinear least-square fitting for all data including both forward and reverse configurations. The uncertainty associated with the noise-temperature measurement is used as the fitting weight for the corresponding data set. The fitted X parameters are finally converted to IEEE parameters, according to their relationship presented in [10].

Fitted results of the LNA at integer frequencies are shown in Fig. 6(a) and (b). The error bars indicate the overall standard

Authorized licensed use limited to: NIST Researchers. Downloaded on May 11, 2009 at 18:27 from IEEE Xplore. Restrictions apply.

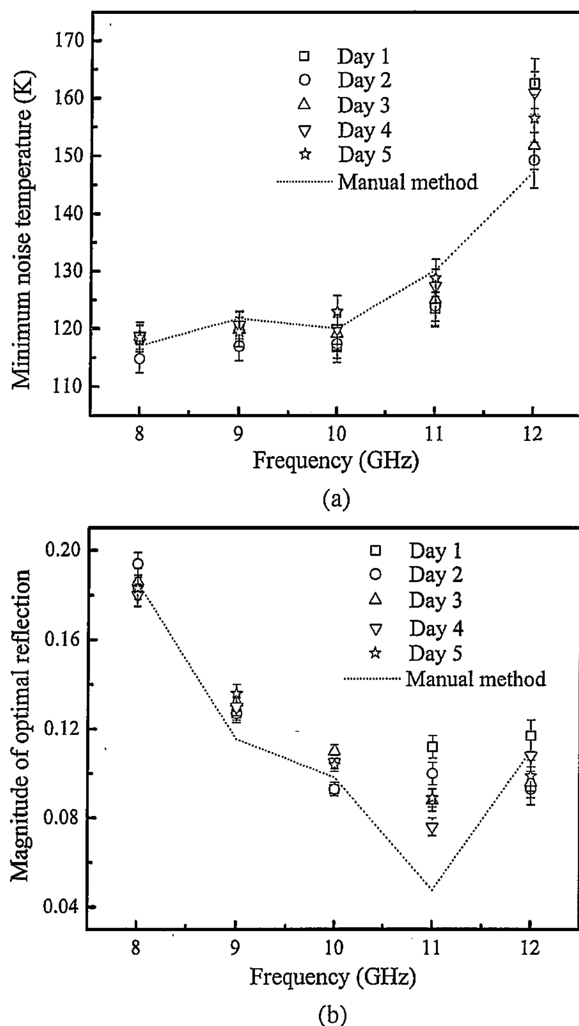

Fig. 6. Fitted results of (a) LNA $T_{\min}$ and (b) LNA $|\Gamma_{\mathrm{opt}}|$ from five days of VTU measurements. The error bars indicate the standard uncertainty (1σ). (Dotted line) Fitted result of the manual method. A fairly good agreement is observed for all measurements.

deviation, which is a combination of types-A and B uncertainties. Type-A uncertainty is the direct outcome of the least-square fitting program. Type-B uncertainty is evaluated through an improved Monte Carlo simulation program [10]. The uncertainties in $T_{\min}$ at all frequencies are below 3%, which is an improvement of more than a factor of 3 with respect to the previous result [6]. Here, we note that the uncertainty presented in [6] was mishandled and should be three times larger than the error bars in the plot. Some of the improvement in the noise-parameter fit is due to an improved treatment of the attenuator in the uncertainty analysis [10], but a significant amount of the reduction in the overall uncertainty is attributable to the improved VTU.

We performed the same noise-parameter measurements over five days. The comparison of fitted results shows a good agreement between different days, which indicates the high repeatability of our measurement instrumentation and verifies the VTU method. A slightly large discrepancy ($\sim$2 K) for $T_{\min}$ at 12 GHz between five-day measurements may be due to larger noise resistance R_n at high frequencies, resulting in a higher output noise power from the LNA. The fact that we were able to perform a full set of measurements in less than a day represents a major savings of time, compared with the manual method, which would require at least a week for a set of measurements.

V. Discussion and Conclusion

The accuracy of the VTU measurement was further confirmed by checking the LNA with the manual method. Both the VTU and manual methods predict the same trend of $T_{\min}$ as a function of frequency, as shown in Fig. 6. The growth of the minimum noise temperature with increasing frequency matches the noise figure specification provided by the manufacturer of the LNA. In addition to the measurement error, the drift of the packaged LNA is noteworthy. We have observed a long-term ($\sim$3 years) drift of more than 1-dB change in the LNA gain. For the time duration of this work, the gain of the LNA has changed by about 0.01 dB (0.2%), which is within the measurement uncertainty.

The extension of the VTU architecture to higher frequencies can be implemented using the components of the right types of connectors. For example, electromechanical switches are available in the PC-2.4 connector format with its operating frequency of up to 50 GHz. PC-2.4 switches exhibit a similar repeatability performance as PC-3.5 switches. Although PC-2.4 switches produce more attenuation at higher frequencies, the higher insertion loss will not substantially limit their capability of the impedance coverage on the Smith chart.

In conclusion, we have successfully upgraded the measurement capability for noise parameters with a newly designed VTU. The VTU exhibits highly repeatable performance and provides an automated and accurate measurement solution. The time efficiency has improved by at least a factor of 5, compared with that of the manual method. In addition, the new method eliminates the measurement error arising from multiple connections and random drift from day to day. The VTU is a fully stand-alone module and can easily be operated in different places. Although the result shown in this paper is in the frequency range of 8–12 GHz, the VTU will function well in the entire design frequency range of 1–12.4 GHz. We also expect that the VTU is adaptable for use in on-wafer measurements and can help mitigate the problems that we encountered in the previous characterization of transistors [4].

Acknowledgment

The authors would like to thank R. L. Billinger of NIST, Boulder, CO, for his suggestions on the VTU design and M. Garelli of the Dipartimento di Elettronica, Politecnio di Torino, Torino, Italy, for the useful discussion on VNA and noise measurements.

References

[1] J. Randa, E. Gerecht, D. Gu, and R. L. Billinger, "Precision measurement method for cryogenic amplifier noise temperatures below 5 K," *IEEE Trans. Microw. Theory Tech.*, vol. 54, no. 5, pp. 1180–1189, Mar. 2006.

[2] S. Long, L. Escotte, J. Graffeuil, F. Brasseau, and J. Louis, "On-wafer noise characterization of low-noise amplifiers in the Ka-band," *IEEE Trans. Instrum. Meas.*, vol. 52, no. 5, pp. 1606–1610, Oct. 2003.

Authorized licensed use limited to: NIST Researchers. Downloaded on May 11, 2009 at 18:27 from IEEE Xplore. Restrictions apply.

[3] T. Gaier *et al.*, "Measurement of a 270 GHz low noise amplifier with 7.5 dB noise figure," *IEEE Microw. Wireless Compon. Lett.*, vol. 17, no. 7, pp. 546–548, Jul. 2007.
[4] J. Randa and D. K. Walker, "On-wafer measurement of transistor noise parameters at NIST," *IEEE Trans. Instrum. Meas.*, vol. 56, no. 2, pp. 551–554, Apr. 2007.
[5] D. Wait and J. Randa, "Amplifier noise measurement at NIST," *IEEE Trans. Instrum. Meas.*, vol. 46, no. 2, pp. 482–485, Apr. 1997.
[6] D. Gu, D. K. Walker, and J. Randa, "Noise-parameter measurement with automated variable terminations," in *CPEM Conf. Dig.*, 2008, pp. 706–707.
[7] G. F. Engen and C. A. Hoer, "Thru-reflect-line: An improved technique for calibrating the dual six-port automatic network analyzer," *IEEE Trans. Microw. Theory Tech.*, vol. MTT-27, no. 12, pp. 987–993, Dec. 1979.
[8] C. A. Grosvenor, J. Randa, and R. L. Billinger, "Design and testing of NFRad—A new noise measurement system," Nat. Inst. Stand. Technol., Boulder, CO, NIST Tech. Note 1518, Mar. 2000.
[9] S. Wedge and D. Rutledge, "Wave techniques for noise modeling and measurement," *IEEE Trans. Microw. Theory Tech.*, vol. 40, no. 11, pp. 2004–2012, Nov. 1992.
[10] J. Randa, "Uncertainty analysis for NIST noise-parameter measurements," *IEEE Trans. Instrum. Meas.*, to be published.

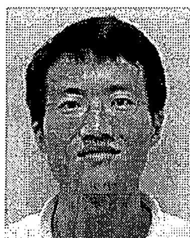

Dazhen Gu (S'01–M'08) received the Ph.D. degree in electrical engineering from the University of Massachusetts, Amherst, in 2007.

Since November 2003, he has been with the Electromagnetics Division, National Institute of Standards and Technology (NIST), Boulder, CO. During his first three and a half years at NIST, he worked on his doctoral research on the fabrication and characterization of hot-electron bolometer devices and the development of terahertz imaging systems. In May 2007, he joined the Microwave Measurement Services Project, where he has been involved in microwave metrology, in particular, thermal noise measurements and instrumentation and fabrication of on-wafer devices for ultrawideband material calibration and nanowire characterization.

David K. Walker (S'82–M'83–SM'07) received the B.A. degree in physics and mathematics from Hastings College, Hastings, NE, in 1980 and the B.S. and M.S. degrees in electrical engineering from Washington University, St. Louis, MO, in 1982 and 1983, respectively.

He spent eight years in industry, working on microwave semiconductor device design and fabrication, before joining the Electromagnetics Division, National Institute of Standards and Technology (NIST), Boulder, CO, in 1991, as part of the Monolithic Microwave Integrated Circuit (MMIC) Project in the Microwave Metrology Group. His work at NIST has included semiconductor fabrication, network analyzer calibration, and on-wafer measurements. He is the holder of five patents related to microwave technology. His current research interests include microwave thermal noise measurements, amplifier and transistor noise-parameter characterization, and calibration of microwave radiometers for remote sensing.

Mr. Walker chairs the Automatic RF Techniques Group Education Committee.

James Randa (M'84–SM'91) received the Ph.D. degree in physics from the University of Illinois, Urbana, in 1974.

He then held postdoctoral and/or faculty positions at the Texas A&M University, College Station; the University of Manchester, Manchester, U.K.; and the University of Colorado, Boulder. During this time, he worked on the phenomenology of elementary particles and the theories of fundamental interactions. Since 1983, he has been with the Electromagnetics Division, National Institute of Standards and Technology (NIST), Boulder. From 1983 to 1994, he was with the Fields and Interference Metrology Group, NIST, where he worked on various topics in electromagnetic interference metrology. From 1994 to 2008, he was with the RF Electronics Group, NIST, where he worked on thermal noise metrology. In 2008, he retired from NIST. He is currently a Guest Researcher with NIST and a Senior Research Associate with the Department of Physics, University of Colorado.

Dr. Randa has chaired the High-Frequency Working Group (GT-RF) of the Consultative Committee on Electricity and Magnetism since 2002.

Authorized licensed use limited to: NIST Researchers. Downloaded on May 11, 2009 at 18:27 from IEEE Xplore. Restrictions apply.